CONTRACT NAS-9-11609

FINAL REPORT

March 10, 1971 through July 31, 1975

CONTRACT NAS-9-11609

FINAL REPORT

March 10, 1971 through July 31, 1975

TABLE OF CONTENTS

INTRODUCTION

A series of four projects involving cardiovascular instrumentation were conducted under Contract NAS 9-11609 during the period 3-10-71 through 7-31-75. The work was performed by the Biomedical Engineering Division of the Harvard Medical Unit at Boston City Hospital in collaboration with Professor Stephen K. Burns' group at M.I.T.'s Research Laboratory of Electronics. The major projects were:

1) The development and ultimate delivery to NASA of a three-dimensional display measurement system for vectorcardiograms.

2) The development and delivery to NASA of a cardiovascular monitoring system to noninvasively monitor beat-by-beat blood pressure and heart rate using aortic pulse wave velocity.

3) The development and delivery to NASA of software for an interactive system to analyze systolic time interval data.

4) The development of microprocessor-based physiologic instrumentation, focussing initially on EKG rhythm analysis.

This report will briefly describe each project, and will include as appendices more complete documentation of the details of the various projects.

I. VECTORCARDIOGRAPHIC DISPLAY AND MEASUREMENT SYSTEM

The fundamental theoretical basis of vectorcardiography is Einthoven's "dipole theory" which states that the electrical field generated by the heart is equivalent to that produced by a simple dipole with fixed origin and time-variant magnitude and direction. Resulting potentials are obtained from the body surface by means of multiple recording leads that are algebraically

combined to produce three signals that are more or less orthogonal. These signals represent the projection of the equivalent electrical vector onto the axes of an orthogonal coordinate system. In standard clinical vectorcardiography, pairs of these signals are used as horizontal and vertical deflection of an oscilloscope beam that thus displays a point representing the projection of the vector on the frontal, horizontal, and sagittal plane. The QRS complex, representing ventricular depolarization, occurs in approximately 80 ms. Hence direct writers are unfeasible and to get hard copy of a record requires an intermediate photographic process.

Under contract NAS 9-11609 we have developed a vectorcardiographic display and measurement system using our general-purpose programmable laboratory computation system which is described in more detail in Appendix IA. The VCG display system is capable of acquiring and displaying VCG's in an extremely flexible manner. It can produce three-dimensional perspective images which can be rotated in arbitrary directions, and can make a quantitative examination of VCG data including calculation of loop areas, mean loop axis, and amplitude and angle of the vector at any instant. In addition it can synthesize the 12-lead scalar EKG from the VCG (assuming a dipole model.)

A detailed description of the initial system including the basic algorithms employed was prepared by Mr. Jerome Sheridan and is presented in Appendix IB. Sheridan's work was extended somewhat to create the final system which was delivered to NASA in 1973.

Operation of the system includes three basic processes: signal acquisition, scalar display, and vector display. Having acquired a signal, the operator can readily switch between scalar and vector display modes; and in the vector mode, he has the option of selecting a three-dimensional perspective presentation that may be viewed with special glasses. Normal presentations are on an oscilloscope, but all displays may be presented on an X-Y plotter for permanent records.

In the signal acquisition process, the X, Y, and Z signals are sampled by a standard clinical vectorcardiograph machine (1000 samples/s). The samples are then stored in the system's core memory. Front-panel knobs allow establishment of a threshold on one of the channels. When the signal exceeds this threshold, an adjustable number of additional samples are stored and these, together with the previously acquired points, form the 1000-point record that will be displayed. This phase also has provisions for calibration and normalization of the three leads.

The scalar display mode presents the stored data on the oscilloscope and allows the user to select a portion of the vector complex to analyze and display as a vector loop. The selected portion is delimited by visible cursors and the time interval between these cursors may be displayed numerically. The first cursor selects the E-point, usually the initial point of depolarization, and this point determines the origin of the orthogonal coordinate system.

In the vector mode, the selected complex is displayed on the oscilloscope in three-dimensional form with provision for rotating the viewing position by means of front-panel knobs.

CURSOR WIDTH 462
MEAN VECTOR: 58, 105
AREA: 25321
POINTER ANGLES: 72, 122
MAGNITUDE: 267 , SAMPLE NO. 254

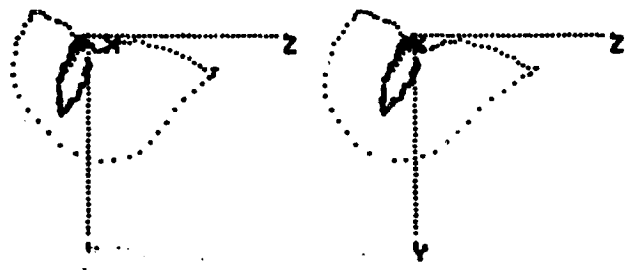

Fig. 1 Normal Sagittal Plane Vector Loop

The standard clinical views, frontal, horizontal, and sagittal, may be selected by means of front-panel switches. Available numerical data include the projected area delimited by a displayed loop, and the mean vector of the loop. A visible pointer representing the instantaneous vector may be superposed and positioned by the operator to any displayed point. The angle, magnitude, and latency (relative to the E-point) of this vector may be displayed.

Other features include adjustable magnification of the vector loop and optional display of 1-mV calibration marks on on the three orthogonal axes. By allowing examination of a magnified view of only the initial portion of the loop, the system provides more detailed information on the important initial forces of depolarization than can be obtained by standard

vectorcardiograph techniques.

Recent trends in clinical vectorcardiography indicate that the full potential of this technique for improved diagnosis will depend on quantitative analysis of vectorcardiogram data. The VCG Display System provides a unique combination of flexible quantitative capabilities, as well as the stereo three-dimensional perspective display of the vector loops. Preliminary clinical trials, conducted with data from selected patients at Boston City Hospital who had a variety of abnormalities, suggest that the system enhances the qualitative differentiation of the vector loop, as well as quantitative analysis. In these cases several characteristics of potential diagnostic value were studied. The relative planarity of normal loops compared with abnormal loops could be readily appreciated and quantitated. In certain cases of myocardial infarction, stereo viewing of the loop, with exam-

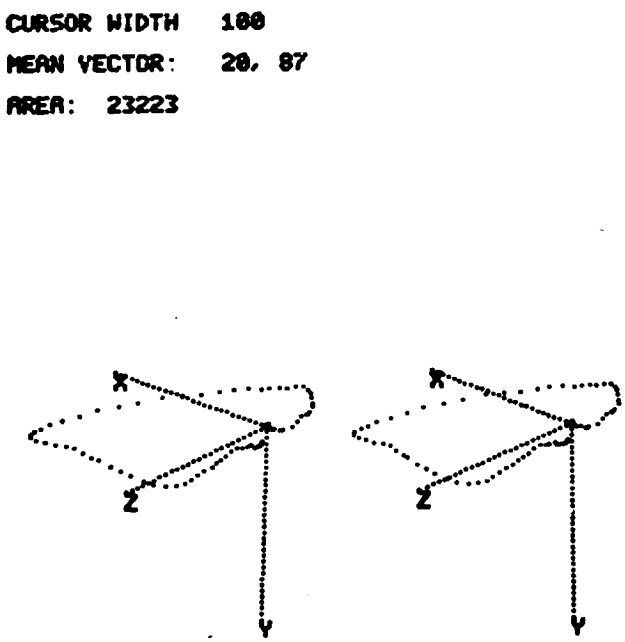

Fig. 2 Rotated three-dimensional vector loop.

ination from several viewpoints, disclosed alterations that are not ordinarily found in the standard planes. The three-dimensional capability provides a more unified representation of the cardiac dipole than is obtained by using 3 orthogonal planar component views, and may assist in revealing new criteria relevant to diagnosis.

Examples of the output from the VCG Display System, recorded on an X-Y plotter, are shown in Figs. 1 and 2. Figure 1 shows a standard sagittal plane vector loop from a normal person. Data specifying width of the vector complex, the projected planar area, the mean vector, and the instantaneous vector (254 ms from the E-point) are presented at the top of the display. Figure 2 shows a rotated view of the same person's vector. These figures are normally viewed with stereo glasses, but some observers are able to achieve the three-dimensional effect by crossing their eyes.

II. CARDIOVASCULAR MONITORING SYSTEM FOR NON-INVASIVE MEASUREMENT OF HEART RATE AND BLOOD PRESSURE.

During the two year period 1971-1973 exploratory research was performed relating to the feasibility of developing an instrument to estimate blood pressure non-invasively using pulse wave velocity as the measured variable. It has been known for many years that the velocity of pulse wave propogation in the arterial system is a function of the elastic properties of the vessel walls: the stiffer the walls, the faster the pulse wave propogation. The speed of propogation of the pulse-wave in thin-walled elastic vessels is given by a form of the Bramwell-Hill equation:

$$V = \frac{3.57}{\sqrt{D}} \qquad (1)$$

where V is the pulse-wave velocity in meters/second, and D is the "distensibility" of the vessel defined as the percentage change in arterial volume per multimeter of mercury change in transmural pressure.[1]

From experimentally determined pressure-volume curves of the aorta it is possible to use Eq.(1) to derive a theoretical relationship between pulse wave velocity and pressure (See Fig. 3).

Figure 3

(From King, A.L., Waves in elastic tubes: velocity of pulse waves in large arteries. J. Appl. Physics 18 595, 1947.)

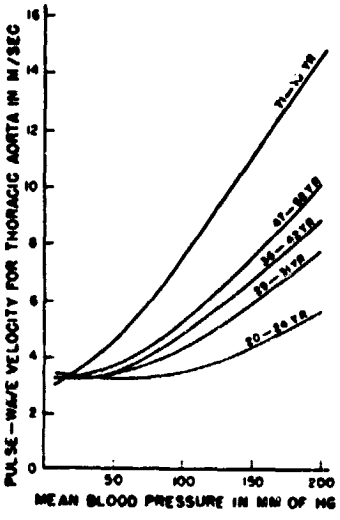

The curves are approximately linear for mean pressures above 70 mmHg:

$$P = K_1 v + P_o \qquad (2)$$

K_1 and P_o are constants which vary with an individual's age and vessel characteristics. In general these constants do not change in a given subject over a period of many months.[2,3,4]

Since smooth muscle tone may greatly affect vessel distensibility, Eq.(2) holds best for the aorta whose wall has relatively little smooth muscle.[6] LaBresh has shown that in dogs the relationship between the foot-to-foot pulse-wave velocity (measured between the arch of the aorta and the femoral artery) and diastolic blood pressure was approximately linear, and that it held under varying conditions such as vaso-constriction, vasodilation, and hypovolemia.[2] Other investigators have demonstrated good correlation between diastolic blood pressure and pulse-wave velocity measured between carotid and femoral arteries in human subjects.[7,8] They used mechanical displacement transducers to detect the carotid and femoral pulses, and measured the delay between their on-sets.

A more complete description of our early experimental work including the literature search is found in the document by Kenneth LaBresh included here as Appendix II-A. The theoretical linear relation between blood pressure and pulse wave velocity was verified in animal experiments using dogs. Figure 4 shows one set of data from LaBresh's experiments, demonstrating the relation between carotid diastolic pressure and the inverse of pulse propogation time between aortic arch and femoral artery.

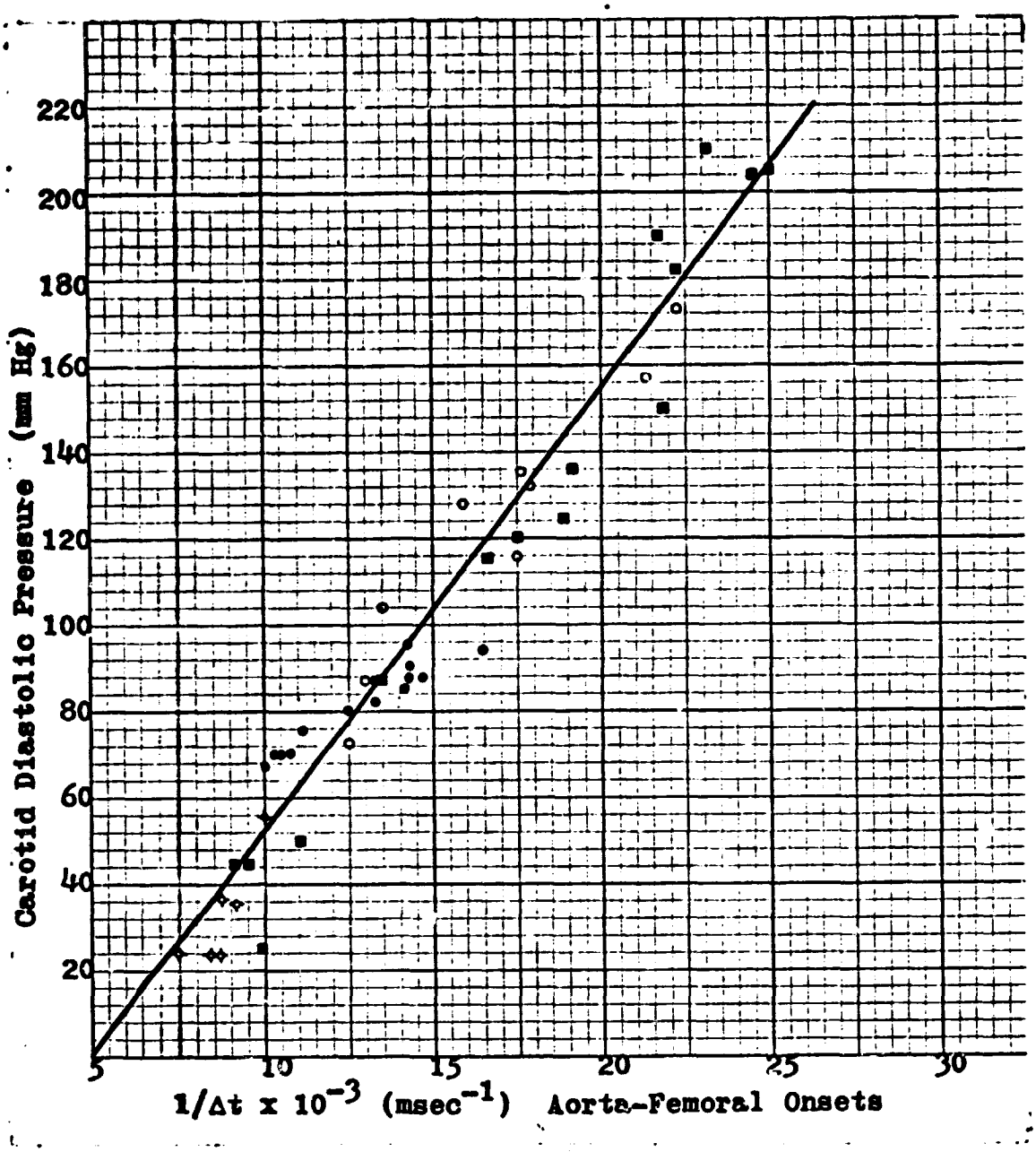

FIGURE 4. Plot of carotid diastolic pressure versus the inverse of the time interval between the onset of the pulse wave in the aorta and the onset in the femoral artery. Data taken under various conditions from Experiment I (✦ = hypovolumia, · = normal, ■ = epinephrine, o = Levophed). Best-fit line: $P = 1.02 \times 10^4 (1/\Delta t) - 5$..07, $\sigma = 11.75$.

The early animal experiments were next extended to human subjects using normal volunteers. Brachial intra-arterial pressure and carotid-femoral pulse wave propogation times were measured. Blood pressure was varied using isometric exercise and inhalation of amyl nitrite. Typical experimental data relating diastolic arterial pressure to the inverse of carotid-femoral pulse-wave propogation time are shown in Figure 5. More complete discussion of this series of experiments is contained in Appendix II-B of Harvey Goldberg.

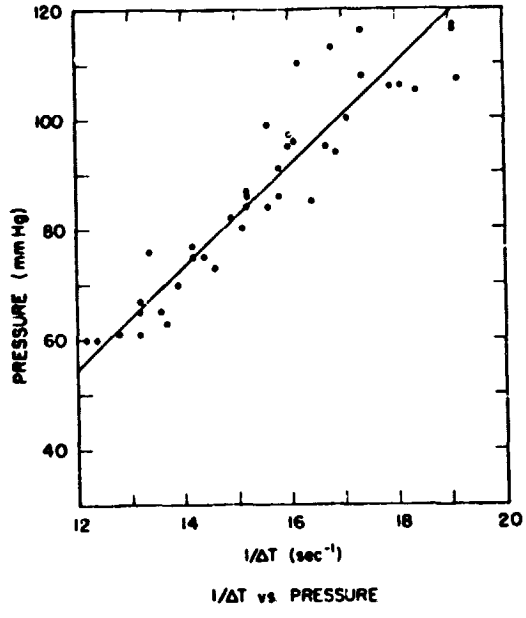

Figure 5

In view of the animal and human data, it seems appropriate, as a first approximation, to consider arterial pressure a linear function of the inverse pulse propogation time ΔT.

$$P = K_2 \frac{1}{\Delta T} + P_o \qquad (3)$$

Again, K_2 and P_o are constants which vary from individual.

Assuming that one could reliably detect the onset of the pulse wave in the carotid and femoral arteries, equation(3)could be used to estimate blood pressure on a beat by beat basis. Ideally the technique could permit non-invasive blood pressure monitoring in ambulatory patients. The biggest problem in realizing such an instrument is the development of pulse wave transducers which are relatively immune to motion artifacts. We considered and tested a number of different transducers, but were unsuccessful at developing a transducer scheme reliable for ambulatory subjects. (A review of the various transducers is contained in Appendix II-C by Donald Gorelick.) A contact microphone proved to be a reasonably good pulse-wave transducer for quiet subjects, however, and served as the basis for the cardiovascular monitoring system (CMS) ultimately developed and delivered to NASA in 1974 for use in LBNP experiments.

The CMS is an analog processor which calculates Eq.(3)on a beat-to-beat basis. The pulse waves are detected using crystal contact microphones which are positioned firmly against the skin over the carotid and femoral arteries. The resultant signals are amplified, differentiated, and then filtered to reduce the amplitude of base-line shifts, movement artifacts, and other noise. Further noise reduction is obtained by gating the pulse signals with the EKG. The instrument is sensitive to inputs from the carotid transducer only during the interval which begins 60 msec after the QRS and ends after a carotid pulse is detected, or 200 msec. after the QRS, whichever comes first.

A principal task of the CMS is to accurately determine the onset times for both carotid and femoral pulses. Both the pulse wave signals and their derivatives are used. The time at which the derivative crosses an operator-selected threshold defines a possible pulse wave onset. If the original pulse wave signal crosses a preset threshold (60% of its average peak level) before the derivative returns to zero, the pulse-detection algorithm is satisfied and a marker pulse is generated.

The interval between carotid and femoral onsets is measured by counting pulses from a crystal controlled clock and storing the resultant binary number, ΔT. The delay time ΔT is then both reciprocated ($\frac{1}{\Delta T}$) and converted to an analog voltage by a reciprocating D to A converter. Finally, constants K_2 and P_o are introduced according to Eq.(3) to provide a calibrated output. The beat-by-beat heart rate is determined from either the EKG or a pulse wave signal using the same clock and a similar reciprocating D/A converter. Figure 6 shows the CMS blood pressure output versus the intra-arterial pressure of an experimental dog. Appendix II-D contains a complete description of the cardiovascular monitoring system including circuit diagrams and operating instructions.

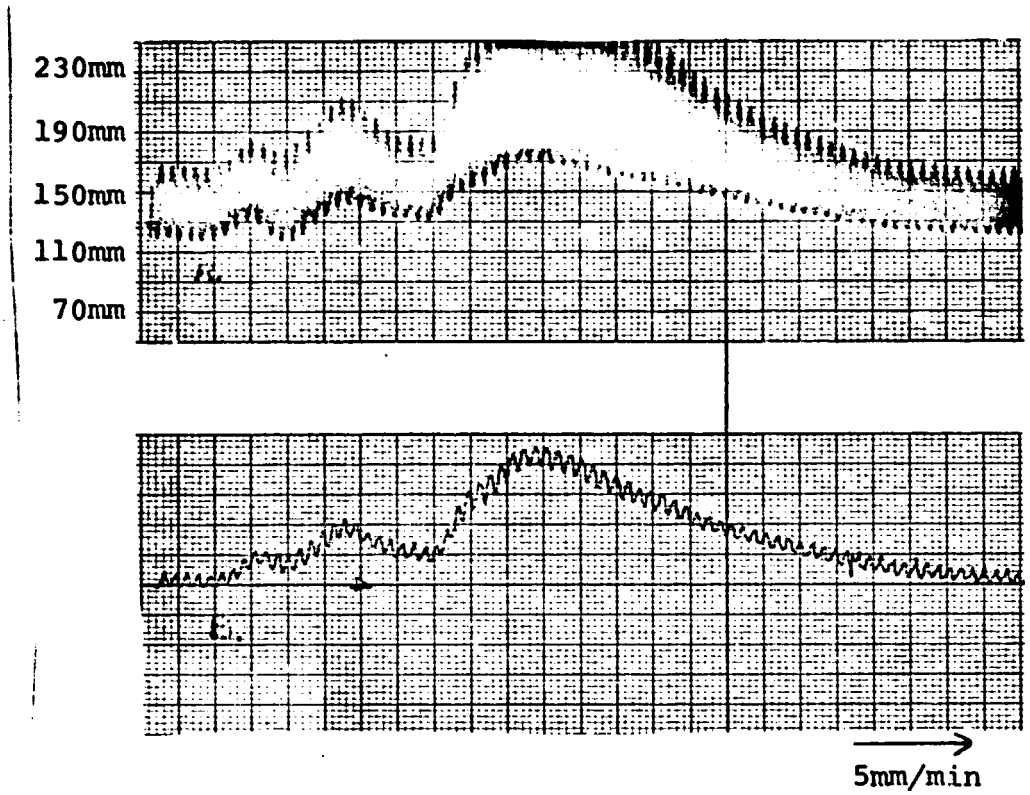

Administration of Levophed

Figure 6

A. Intra-arterial BP in a dog.
B. Output from the CMS BP Channel. (See Text.)

III. MICROPROCESSOR-BASED PHYSIOLOGIC INSTRUMENTATION

Objectives

The objective of this work has been the evaluation of a universal physiological instrumentation system incorporating dedicated programmable microprocessors. We envision a modular system, in which each module (with its own data processor) would be dedicated to a specific task such as arrhythmia monitoring, control of experimental apparatus, generation of displays, etc. While the specific function performed by each unit would be different, the units would be constructed on a common hardware base. For example, a unit could become an arrhythmia monitor by software changes, not hardware modifications. Each module would contain an integrated circuit CPU, read only memory, read/write memory, a communications link (to other modules or a larger computer),plus any specific peripherals not included as part of base module.

The scheme of implementation allows the development of a common hardware base (perhaps as small as a single card of electronics) which can be thoroughly tested and certified. These basic modules would be inventoried for programming to perform specific experiments or tasks.

The effort described in this section is continuing under a new contract, number NAS 9-14618 from JSC to Beth Israel Hospital.

The Portable EKG Processor

We selected the development of a portable EKG monitoring system as a specific task to prove the concept of programmable instrument modules. The instrument will examine each QRS complex, categorize it by timing and width, and provide a summary of cardiac shythm over a 24 hour period. The unit is battery operated and may be carried by the subject during normal daily activities. This task was chosen because its requirements are relatively demanding. For the unit to be carried by a subject, it must be physically small, consume minimum power, and communicate on a periodic basis with another processor to receive programs and transmit reports of the subject's status.

The system uses an INTEL 8080 microprocessor which has 8-bit arithmetic operations, interrupt capability, and a hardware stack facility. A non-portable 8080 processor system has been constructed for use in software development. An assembler (Appendix III-A) which executes on the NOVA line of minicomputers has been developed for the 8080, which permits a major portion of the software development to be done on an established system. A debugger which executes on the nonportable system has also been developed. This debugger provides facilities to control and monitor program execution as an aid to 8080 software development.

Portable Processor Hardware

A block diagram of the portable system is provided in Figure 7. The hardware consists of six major functional components:

- the microprocessor with bootstrap read-only memory
- program and data storage memory

- analog-to-digital converter and EKG amplifiers
- real time clock
- bit serial input/output
- power source

Physically, the unit is being constructed in a metal chassis, 1-3/4 x 6 x 9-3/4 inches.

The unit is constructed on three 4½ x 6 inch cards, with additional smaller cards for the power supply converter and the front panel interface. The chassis is completed.

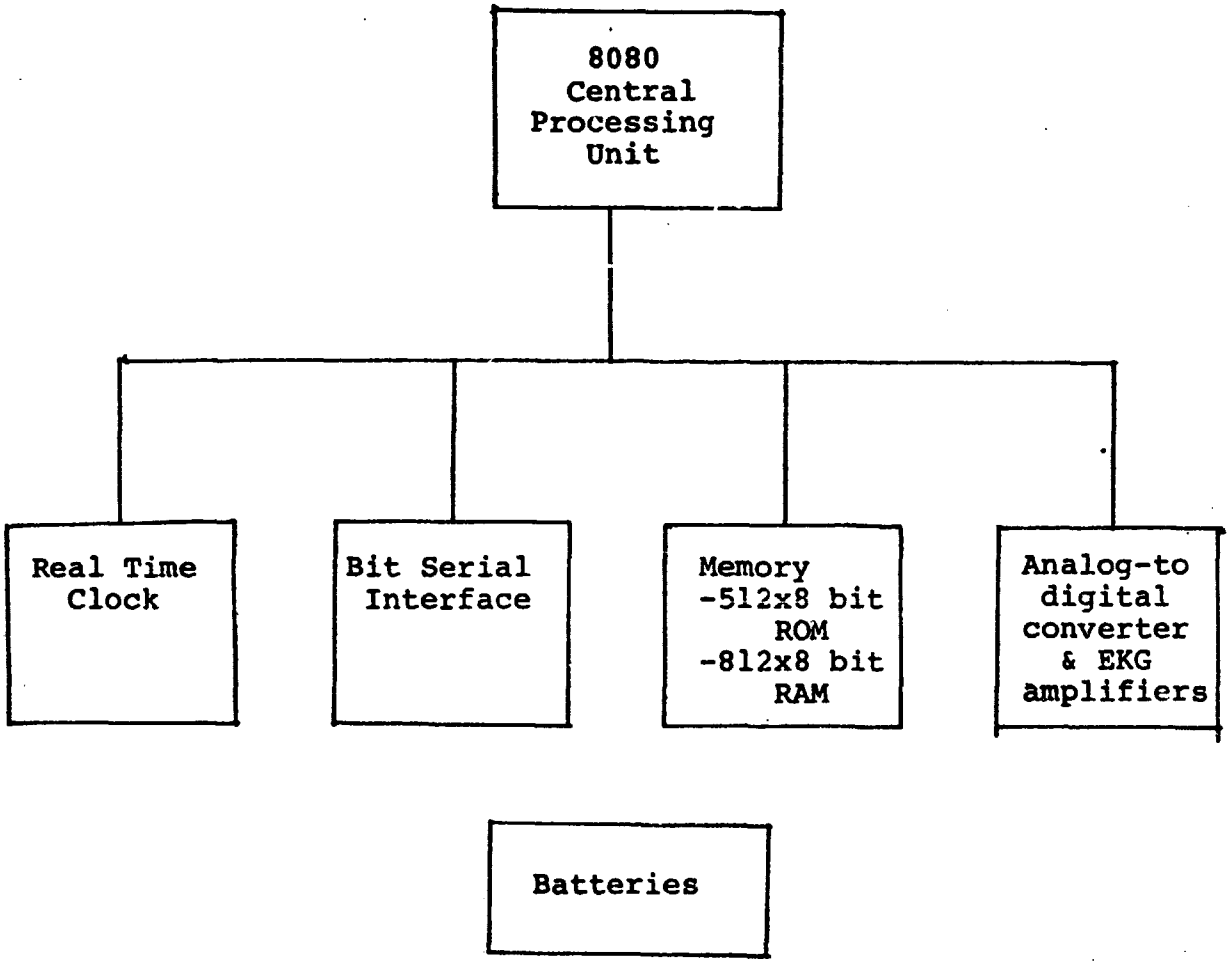

Figure 7 - Block Diagram of Portable Processor

The processor card contains the 8080 Central processing unit (CPU) and its required support circuitry. This card is complete and is currently being tested. In addition to the CPU, it contains 512 8-bit words of read-only memory, (ROM), the CPU crystal clock with driver circuitry, the CPU status-logic required to interface to memory and perpherials, and the power on/off sequencing logic. The ROM provides storage for the bootstrap program which receives initial control of the CPU when power is first turned on in the system. This program communicates with the NOVA system to obtain the program to be executed by the processor. In addition, the ROM contains a program which responds to the real time clock and maintains the time of day. The crystal clock is a 16 megahertz oscilator which provides the CPU with pulses determining the timing of instruction execution. The CPU status logic controls and monitors the status of the CPU, deriving timing information and control pulses for the memory and peripherals in the system. The power sequencing logic provides an orderly turn on and turn off of the CPU and its support logic. To conserve power, all of the logic on the processor card is turned off when not actually needed. In the present system, the CPU will be powered up 250 times per second. A program in ROM will receive machine control and check the status of the system. If required, the CPU will remain on to process data, if not the CPU will request that its power be turned off. Approximately 16 microseconds are required to restart, or shut off, the system; thus the overhead of powering up and down is about 3/4 of one percent of available CPU time.

The memory card will contain 8192 8-bit words of random access read-write memory (RAM.) The memory is being implemented with Texas Instruments 4096 bit dynamic RAMs. Dynamic RAMs store the digital data in the form of charge on capactors, thus if the power is removed data is lost. In addition, the charge leaks off the capacitors requiring that it be periodically refreshed. The selected RAMs require that they be refreshed every 2 milliseconds and refreshing requires 64 operations on the memory, thus the time between refresh operations is 31.25 microseconds. Special circuitry on the memory card will assure that the memory is refreshed, and that the refresh operations do not interfere with normal operation of the CPU. A clock is required to time the memory refresh operation, so this clock will also serve as the real-time clock to provide time of day information to the CPU. The memory card has been designed, and debugging will proceed as soon as the CPU card is fully operational.

The third system card contains an analog-to-digital converter, an EKG preamplifier, and a bit serial input-output port to communicate with an external modem. The EKG amplifier provides gain to shift the levels of the EKG to those compatable with the Analog-to-digital converter (A-D). The A-D is a integrated circuit fabricated to require low power of operation. It can convert a sample in 20 microseconds, and its power may be switched on and off by the CPU. The bit serial input-output port provides a serial stream of data which allows communication with another processor. The card is designed, and is currently being tested.

Power to the other cards in the system is provided by lithum primary cells and a DC-to-DC converter. The converter provides output voltages of +12 volts and -9 volts from the primary power source of 5 volts. The primary power source is a pair of "D" size lithum cells. These cells provide 8 ampere-hours at a nominal 2.8 volts. The converter card has been fabricated on a printed circuit card and tested at a full load of 2 watts. The efficiency of the converter exceeds 80% and about 1/2 of the total power will be derived directly from the batteries (100% efficiency), so the total system efficiency will be greater than 90%. This provides a total of 40 watt hours for the system. With the estimated average load of 300 milliwatts, the system could run for about 120 hours (5 days).

Portable Processor Support Software

An assembler which executes on the NOVA line of minicomputers has been developed for the 8080, which permits a major portion of the software development to be done on established systems. The assembler (Appendix IIIA) is a two-pass assembler implemented in NOVA assembly language. ASM80 accepts assembly language statements as input and produces absolute binary as output. The assembler allows direct access to the full order code of the 8080. In addition to machine instructions, the assembler will accept various psuedo instructions to direct its operation.

The non-portable 8080 system includes a debugger which provides powerful program diagnostic aids similar to those provided by the NOVA debugging system. This debugger uses a combination of hardware and software to control and monitor the flow of program execution in the 8080.

Portable Processor Applications Software

The core of the monitoring system is the arrhythmia analysis routine executed by the processor. The algorithm will be similar to that described in Nolle and Clark.[9] At present the algorithm is being implemented in ALGOL on a NOVA system.

After debugging and evaluation, the final algorithm will be written in 8080 assembly language for the portable processor system.

A significant fraction of the processor time required for EKG analysis in this algorithm is devoted to preprocessing the data. This preprocessing algorithm has been implemented and tested on the microprocessor system. The algorithm implemented is a Zero Order Interpolator (ZOI). A ZOI represents a waveform as a series of fixed amplitude but variable length segments. The output of this algorithm is a concise description of the EKG that is adequate for further processing to perform arrhythmia analysis. This algorithm was chosen because it is similar to the AZTEC algorithm developed by Cox,[10] and because of our practical experience with the algorithm. (See Appendices III-B and III-C)

The algorithm tracks the minimum and maximum values of the input signal. When the signal excursion has exceeded a specified maximum aperture a new segment of output is created to represent the previous signal data points. The amplitude of the segment is the average of the maximum and minimum value of the input, while the length is specified by the elapsed time since the last segment was output. As each output segment is produced, the maximum and minimum tracking is reset to the current sample value. 56 machine instructions are required to execute this al-

gorithm, requiring approximately 0.2 milliseconds to execute.

The algorithm represents the signal within a specified error tolerance. Thus, with a rapidly changing signal (as the QRS complex) the output segments become shorter until limited by the sampling period. If a signal is not changing rapidly (as the baseline between QRS complexes), the output segments become longer until they limit at the specified maximum allowed length. Unlike conventional sampled representations, the ZOI adjusts its output rate to fit the actual changes in the input data. In the case of the EKG, the ZOI will produce a burst of segments every QRS complex, then produce very few segments in the interval between complexes. The expectation, verified by measurements, is that over an EKG cycle, the average output of data is 5 to 10 times less than in conventional sampling. In practice, this data rate reduction is useful only if the analysis program is capable of handling the segment data as easily as if it were sampled data. Practical experience indicates that this is the case.(Appendix III-C) Figure 8 presents a sampled EKG and the ZOI representation. The full range of the sampled data in the 8080 is 8 bits or 256 levels. In figure 8a, the aperture constant was set at 8 or about 2.3% of the peak to peak range of the QRS complex (3.1% of full scale). With this aperture constant, the comparison with the sampled data is very good. Note that, in most cases, the P wave is easily recognizable in the ZOI representation. As the aperture constant is increased (Figures 8b, and 8c) the fine structure of the EKG disappears in the ZOI representation. With an aperature constant of 16, or about 4.7% of the peak to peak value of the QRS, the P wave is not reliably represented in the ZOI representation.

Figure 8

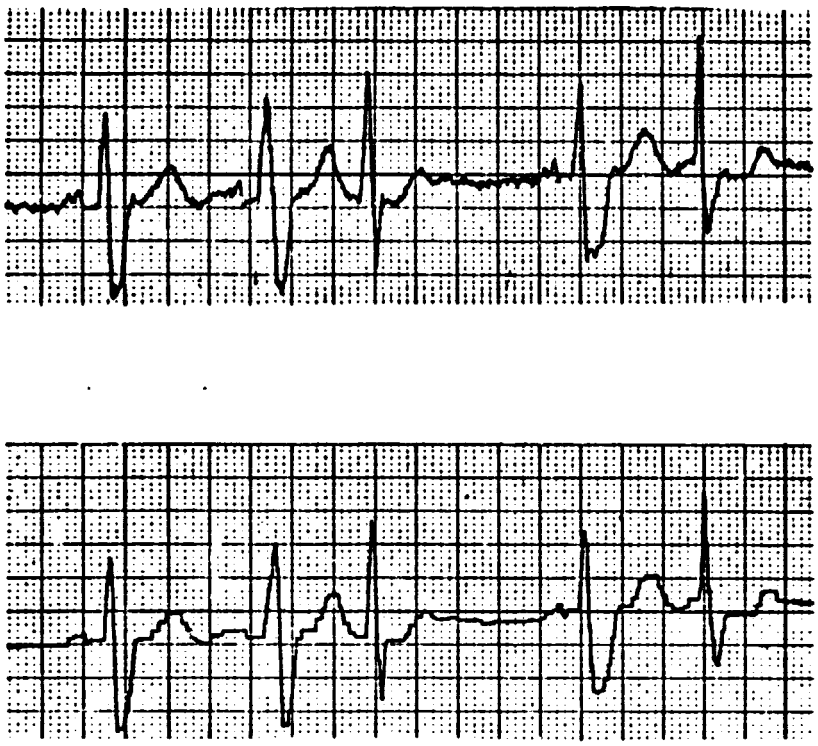

a) Aperture = 8, or about 2.3% of p-p QRS value.

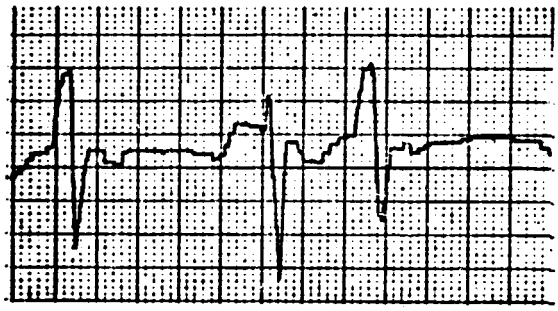

b) Aperture = 12 or about 3.5% of p-p QRS value.

Figure 8

Examples of PMS produced ZOI representation. All data sampled at 250Hz.

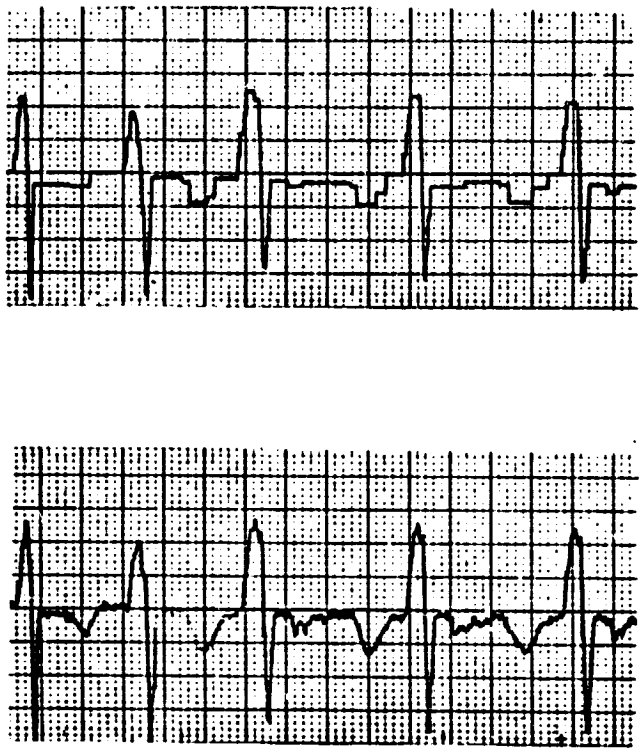

c) Aperture = 16, or about 4.7% of p-p value.

Figure 8 (Continued)

Examples of PMS produced ZOI representation. All data sampled at 250 Hz.

However, the representation would be adequate for arrhythmia analysis and to classify QRS complexes by morphology.

The ZOI algorithm implemented in the 8080 averages less than 3.2% of the processing capability of the system, leaving large reserves of computational power for analysis.

IV. SYSTOLIC TIME INTERVAL MEASUREMENT SYSTEMS

A semi-automatic interactive program for the measurement of systolic time intervals was developed to meet JSC provided specifications. The program was implemented for the 3-D VCG Display Ststem at JSC. Programming was done in NOVA Assembly language and FORTRAN IV. Full source listings of the software were delivered to JSC.

The system samples the EKG, Carotid Pulse, and Phonocardiogram waveforms at 500 samples per second. Respiration is sampled at 62.5 samples per second. The most recent 2 seconds of the EKG and respiration are displayed along with the most recent second of the Phonocardiogram and Carotid Pulse. The operator may control cursors displayed on the data to identify timing landmarks including the onset of the Q-wave in the ECG, the onset of the first heart sound, the onset of the rise of the carotid pressure, and the incisura of the carotid pulse. The program then automatically measures the R-R interval, the left ventricular ejection time, the pre-ejection period and the isovolumetric contraction period.

The program displays the computations and accumulates a statistical summary of the data. Data files may be archived on the mass storage device contained in the VCG system.

PEFERENCES

1. Bramwell, J.D. and Hill, A.V., "The Velocity of the Pulse Wave in Man", Proc. Roy. Soc. Ser B 93: 298, 1922.

2. LaBresh, K., Pulse Wave Velocity as a Measure of Arterial Blood Pressure, S.B. Thesis, Electrical Engineering Department, M.I.T., June 1970. (Included here as Appendix II-A)

3. Hallock, P. and Benson, I.D., "Studies on the Elastic Properties of Human Isolated Aorta", J. Clin. Invest. 16: 595, 1937.

4. Steel, J.M., "Interpretation of Arterial Elasticity from Measurements of Pulse Wave Velocities", Am. Heart J. 14: 452, 1937.

5. Chang, P., "Immediate Smoking Effects as Observed from the Dispersive Nature of Pulse Wave Velocity", 24th ACEMB, Las Vegas, 1971.

6. McDonald, D.A., "Regional Pulse-Wave Velocity in the Arterial Tree", J.Appl. Physiol. 24: 73, 1968.

7. Nielson, L., Roin, J., and Fabricius, J., "Carotid-Femoral Pulse Wave Velocity", J. Am. Ger. Soc. 16: 658, 1968.

8. Goldberg, H., Diastolic Blood Pressure and Pulse Wave Velocity in Humans", S.B. Thesis, Department of Electrical Engineering, M.I.T., January, 1972. (Included here as Appendix II-B.

9. Nolle, F.M., and Clark, K.W., "Detection of Premature Ventricular Contractions Using an Algorithm for Cataloging QRS Complexes, "Proceedings of the San Diego Biomedical Symposium.

10. Cox, J.R., Jr., et al, "AZTEC, A Preprocessing Program for Real-Time ECG Rhythm Analysis", IEEE Transactions on Biomedical Engineering, V. 15 No. 2, April 1968, pp. 128-129.